Diode-laser production of collimated slow cold potassium beams and crossover resonances

Shifang Li and John F. Clauser
Department of Physics, University of California–Berkeley, Berkeley, California 94720
(Received 30 August 1993)

We describe the results of three sets of experiments to investigate producing cold slow collimated potassium atoms for applications with no access available for the introduction of counterpropagating laser light along the exiting atomic beam's axis. Velocity profiles are obtained via fluorescence from $D1$ excitation at perpendicular and nearly parallel incidence by a probe laser. Spatial profiles of both the cold- and residual hot-beam components are measured with a position-scanned hot-wire detector. Velocity-component holes and decelerated cold components are observed, along with direct evidence of perpendicular heating of the cold components. A first set of experiments uses a variant of conventional chirp cooling and/or hole burning. Light is introduced by a heated inclined mirror, while atoms exit through a slit in the mirror. Loss of intensity at low velocity is observed and discussed. A second set of experiments investigates velocity-selective optical-pumping crossover resonances that occur near the mirror, where the incident and reflected beams overlap for several alternative geometries. A third set of experiments investigates cold-beam production using laser-induced velocity selection and deflection. It provides a higher cold-atom intensity, along with the means to perform high-resolution spectroscopy.

PACS number(s): 32.80.Pj, 42.50.−p, 42.55.Px

I. INTRODUCTION

Typical diffraction-grating atom interferometers require a well-collimated slow cold atomic beam [1]. Conventional methods for producing such a beam are attractive for use with alkali metal beams such as rubidium and cesium (e.g., chirp and Zeeman spontaneous-force cooling) in that they can be accomplished using low-cost diode lasers [2]. On the other hand, their use in this application suffers from several major drawbacks. First, they require a laser beam to counterpropagate with the atomic beam. However, the presence of an interferometer that employs microfabricated solid gratings obstructs the introduction of this laser beam. Second, beam blow-up by perpendicular heating sets an effective lower limit to the velocity of a beam produced by these methods, and/or an upper limit to the effective source brightness, without the use of additional perpendicular cooling via molasses. Third, building a longer cooling apparatus so as to allow cooling of a greater fraction of the parent thermal velocity distribution does not increase the resultant cold-beam intensity, since the increased inverse r^2 loss in flux counterbalances the increased cooled fraction of the beam. Finally, if only a fraction of the velocity distribution is cooled and/or decelerated, the resulting beam exhibits a highly nonmonoenergetic velocity distribution.

The first two difficulties can be overcome by simultaneous deflection and perpendicular cooling via the use of molasses [3], by accumulation of atoms in a trap and then either launching them upward [4] or dropping them [5]. Solution of the fourth problem, i.e., separation and dumping of the residual uncooled beam components (which retain the spatial collimation of the parent thermal beam) is also possible by additional collimation. Unfortunately, use of these techniques requires high laser power, many more laser frequencies, careful attention to the local magnetic field geometry, and considerable effort, expense, and complexity. Even then, employing perpendicular cooling with polarization-gradient molasses will produce a cold slow atomic beam with a perpendicular momentum spread equal to that of several photon recoils. Herein we describe a particularly simple solution to the problem that requires only two time-independent laser frequencies in an ambient laboratory magnetic field that produces high source brightness for slow cold atoms with about the same perpendicular velocity spread as that of polarization-gradient molasses.

In our first set of experiments we explore the limitations of conventional atom cooling and deceleration techniques, when applied to potassium [6] and wherein there is no access for introduction of cooling and repumping light along the cold beam's exit. In these experiments (described in Secs. II–IV of this paper) we employ ribbon-focused $D2$ light from two diode lasers, counter-directed on potassium effusing from an oven. The cooling and repumping laser light is introduced by a heated inclined mirror and the cooled atoms exit through a slit in the mirror. Section II of this paper describes our apparatus. Sections III and IV describe our measurements of the resulting velocity and spatial profiles of the exiting beam. Perpendicular heating of the cooled components is evident from the spatial profile measurements made with a scanned hot wire. This heating causes a serious diminution of low-velocity beam intensity.

In Sec. V we discuss the evident loss of intensity of the decelerated cold-beam component at low velocities. We note of these experiments that the intensity of cold "holes" (atoms absent in the parent beam over a narrow velocity band) is significantly higher than the intensity of decelerated cold atoms. Given an observed slight asymmetry in the observed spatial profile we are led to suspect that perpendicular deflection processes may be impor-

tant. Indeed, a simple calculation suggests that perpendicular deflection is a far more prominent process than is longitudinal cooling. Upon considering the various orders of magnitude of the relevant processes, we then anticipate that direct transverse deflection of the beam by laser absorption of a small number of photons will be a far more effective method for producing cold slow beams of both atoms and holes than is longitudinal cooling. A beam of cold atoms can then be made nearly as intense as that of a beam of cold holes.

In Sec. VI we examine another curious feature of the data for the above experiments—strong resonances that occur as a function of laser tuning. We do so in a second set of experiments by reconfiguring our apparatus to apply diagonally incident light only in the vicinity of the mirror. We thus identify the cause as velocity-selective optical pumping crossover resonances and trace the origin to the vicinity of the mirror.

In Sec. VII we discuss a third set of experiments for producing a cold beam of atoms by velocity-selective deflection. In these experiments the cooling and repumping laser optics are reconfigured to apply diagonally incident laser light with no mirror. The experiments demonstrate velocity selection by deflecting a desired velocity component out of the parent beam. The experiments then produce two separated intense beams of both atoms and holes, respectively, each with a quasimonoenergetic spectrum. When perpendicularly incident light from one laser is used, all velocity components are deflected and high-resolution spectroscopy is afforded by the scheme. This last alternative geometry further allows immediate calibration of the laser wavelengths.

While some of our results are readily anticipated from previous work, others may seem surprising. In either case they demonstrate difficulties encountered in trying to generate cold slow beams with a high source brightness, and also demonstrate a simple attractive alternative methodology for doing so. Since previous workers have been concerned primarily with achieving a high flux of cold slow atoms into a large target volume (e.g., that of a trap), the achievement of high source brightness has rarely been a concern, and such difficulties have received minimal attention. Sec. VIII presents a summary and our conclusions.

II. EXPERIMENTAL APPARATUS

The apparatus, configured for use with a heated inclined mirror, is diagrammed in Fig. 1. A vertically oriented stainless steel vacuum vessel is divided into two chambers by a differential-pumping slit, thus forming a source chamber and a beam analysis chamber operating at about 10^{-8} and 10^{-9} Torr, respectively. The lower chamber contains a 450 K isothermal copper oven filled with metallic potassium, whose vapor effuses from a 200 μm$\times$5mm knife-edge slit in the oven's top. The configuration was chosen to minimize the loss of low-velocity components that is observed when a channeled exit is employed [7]. (A partial level diagram for potassium is shown in Fig. 2.)

The cooling apparatus is located in the source

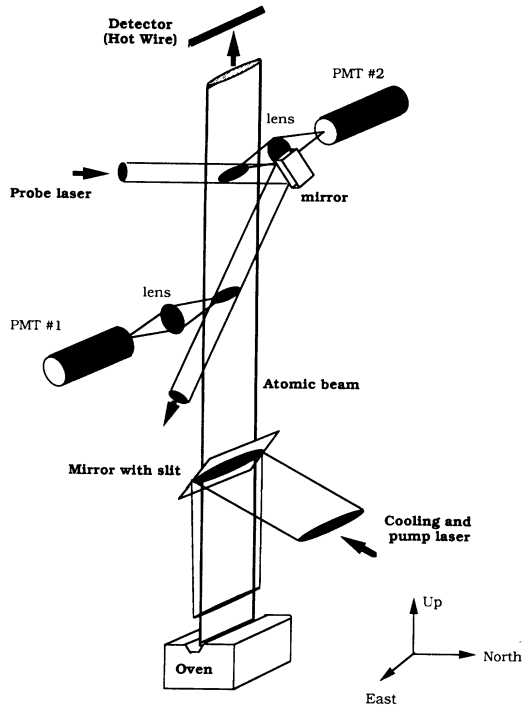

FIG. 1. Geometry of the experimental apparatus.

chamber. Two laser beams, cooling and repumping, are each produced by a diode laser. Both are circularly polarized in the same sense. Each operates in a single unnarrowed mode with a bandwidth of about 15 MHz. The average bandwidth and difference frequency were measured by observing a heterodyne with a fast photodiode and a rf spectrum analyzer. Each is located in a separate vacuum can, is temperature stabilized at about 200 K, with its beam exiting the can through an antireflection-(AR) coated window. Nominally operating at 780 nm and $\leq$25 mW, the low temperature allows the diodes to

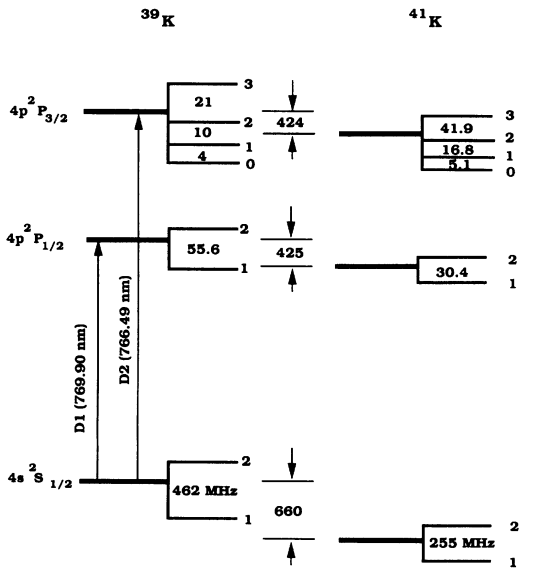

FIG. 2. Isotope shift and hyperfine splittings (in MHz) of ^{39}K (left) and ^{41}K (right) levels associated with the $D1$ and $D2$ lines.

operate at 766 nm, locked to, but tunably offset from, the wavelength of the potassium $D2$ resonance transition, in turn provided by an auxiliary potassium absorption cell. Accumulating the various losses of the system's optics, typically less than 50% of the available laser power is incident on the atoms.

The two laser beams are combined to copropagate, focused with a combination of spherical and cylindrical lenses to form a single ribbon-shaped beam. This beam, in turn, is counterdirected against the atomic beam via a hot ($\approx 100\,^{\circ}$C) inclined, aluminized, and SiO_2-coated silicon mirror. It focuses to form a cylindrical beam waist (in the thin direction) centered on the oven's exit slit, approximately 30 cm below the mirror. At the center of the laser beam the mirror contains a thin knife-edged slit (60 μm$\times$8 mm), beveled on the upper face to allow atoms that have interacted with the laser beams to pass through. The slit is sufficiently thin that the shadow it casts in the laser beam rapidly diffuses away by diffraction in about 1–2 cm, long before the laser beam reaches the oven [8].

The cooling and decelerating mechanisms produce both cold- and residual hot-beam components. To allow us to distinguish these from each other, the lasers are ac modulated at a low audio frequency. Modulation is accomplished either by electrically shifting both laser tunings to nonresonant wavelengths, or by blocking one of the beams with a liquid crystal shutter. The modulation wave form is divided into three periods. During the first period (80 msec) long-term drift of the lasers is stabilized by locking their wavelengths to that of the potassium $D2$ resonance line of an absorption cell. To do so, we apply a square wave frequency dither during the stabilization period to alternately retune the lasers to opposite wings of the absorption line (compensating for laser power variation across the line). We then sample the absorption on opposite wings, and then apply the average difference as slowly varying feedback to the laser injection current to maintain equality of these resulting absorptions. The second period (40 ms) is the "resonant observation period." During this period, the lasers are tuned approximately 437–441 MHz apart—the approximate average frequency of the potassium hyperfine separation. The third period (40 ms) is the "nonresonant observation period." It differs from the resonant observation period in that the lasers are either tuned only about 340 MHz apart, or one of them is blocked by a liquid crystal shutter.

Upon leaving the cooling apparatus, the atomic beam passes through a liquid-nitrogen-cooled baffle and the differential pumping slit. Thence, it propagates upward into the beam analysis chamber, where its velocity distribution and spatial profile are measured. Without the cold baffle, room-temperature potassium is found to migrate into the analysis chamber and interfere with fluorescence measurements. In typical operation the full thermal beam ionized atomic current detected at the top of the chamber by a hot wire with a 1$\times$8 mm frontal area, 1.3 m distant from the hot mirror, is about 1–10 nA ($6-60\times10^9$ atoms per s). Depending on their velocity, slow cold-beam components typically represent less than 1% of this current.

The atomic beam's velocity distribution is measured by observing its resonance fluorescence. The fluorescence is excited by an additional probe diode laser system, similar in construction and wavelength stabilization technique to the cooling and repumping laser systems, but operating at 769 nm, the potassium $D1$ resonance transition. The probe laser beam crosses the atomic beam twice. Each crossing is viewed by a photomultiplier while the laser's wavelength is slowly swept. In addition to the wavelength stabilization feedback to this laser, a second feedback loop is used to linearize the relationship between the laser's wavelength and the sweeping ramp. Both photomultiplier signals are accumulated on a signal averager.

At the first crossing the laser beam is perpendicular to the atomic beam. With this geometry, the Doppler effect is minimal so that, upon scanning the probe laser's wavelength, the potassium hyperfine structure is displayed and resolved in the fluorescence spectrum. This spectrum, in turn, allows calibration of the probe laser's wavelength. It is shown in Fig. 3, along with calculated spectra for comparison. To obtain high spectral resolution, the probe laser must be accurately perpendicular to the atomic beam to prevent Doppler broadening, and attenuated to prevent power broadening (not always the case, but otherwise unimportant for our calibration purposes). The full $D1$ line hyperfine structure of ^{39}K is displayed and resolved, along with that of ^{41}K, which represents about 6% of naturally occurring potassium.

At the second crossing the laser beam is nearly antiparallel to the atomic beam. With this geometry, the Doppler effect is maximal. The beam's velocity profile is then provided as a function of laser wavelength in the fluorescence spectrum. Given the calibration afforded by the first crossing, the velocities of cold features in this spectrum may be measured. Figure 4(a) shows the calculated raw spectrum and Fig. 4(b) shows that obtained at the second crossing with no cooling laser radiation applied. It is composed of the two spectral components produced by the thermal hyperfine level populations—40% of the atoms in the $F=1$ level and 60% in the $F=2$ level. Each component is Doppler shifted by the parent

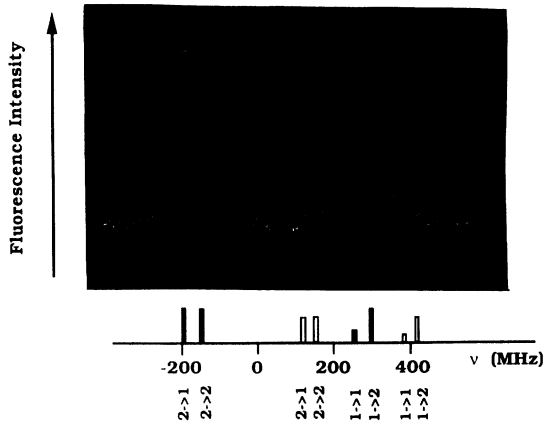

FIG. 3. Upper trace: $D1$ fluorescence spectrum observed at perpendicular crossing used for probe laser calibration. Lower trace: Wavelength reference values for ^{39}K (solid) and ^{41}K (open).

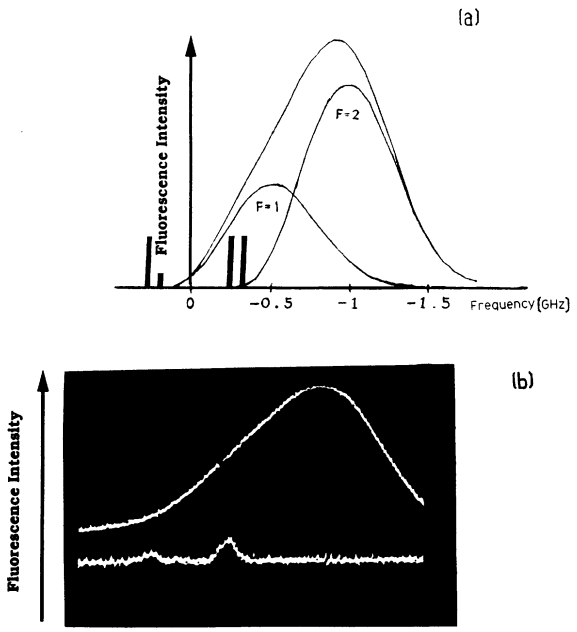

FIG. 4. Thermal parent beam velocity spectrum (a) calculated, and (b) observed in the near-parallel fluorescence with no cooling lasers incident (upper trace), along with the associated perpendicular spectrum used for velocity calibration (lower trace).

thermal beam velocity distribution, and the two components are offset from each other by the average $D1$ potassium hyperfine structure (about 450 MHz $\approx$ 346 m/s). In this spectrum the hyperfine structure is unresolved, and the $F=1$ and 2 distributions overlap.

Distortion of the spectra by the probe beam's causing cycling, optical pumping, and/or additional cooling is minimized by employing the $D1$ line in the probe, by the short atomic transit through the probe in comparison with the probe's sweep rate, and by sweeping the probe from low to high velocity. Unlike the scheme used by Watts and Wieman (see Ref. [2]), which used the retrace of the cooling laser ramp for a velocity probe, our use of an independent probe laser allows us to measure the time-averaged velocity distribution, whereas theirs measured only the velocity at the end of each cooling ramp.

Unfortunately, we find that the unresolved hyperfine structure spectrum displayed at the second crossing is complicated by optical pumping of the beam by the cooling and repumping lasers. Analyses of the raw spectra are complicated by the observation that a depletion of fluorescence at a given velocity component can represent either a mechanical depletion of atoms at this velocity or optical pumping of atoms to the opposite hyperfine state at effectively the same velocity. The latter process is indicated by a corresponding peak in the fluorescence at an apparent velocity one hyperfine structure equivalent velocity offset. To minimize effects of this latter process, up-down gating of the signal averager input is applied. That is, the second crossing's photomultiplier signal is alternately added to and subtracted from the accumulating signal averager spectrum, synchronously during the resonant and nonresonant excitation periods. Discrimination between the two processes is afforded by the fact that optical pumping occurs with far fewer photons than does mechanical cooling, whereupon it occurs well out on the wings of the transition. As a result, optically pumped features appear much broader than do mechanically burned ones. The optically pumped features, by virtue of their much broader bandwidth, then cancel each other via the up-down gating and leave the mechanical effects of narrowband laser velocity manipulation more evident.

III. HOLE-BURNING VELOCITY SPECTRA

To observe velocity hole burning, the laser frequencies are held constant during each of the resonant (and nonresonant) periods. The cold components of the velocity distribution appear as a cold velocity doublet. The doublet consists of a cold "hole" at the laser's equivalent Doppler shifted wavelength, accompanied by a small "refuse" velocity component at an adjacent lower velocity. The second component is composed of atoms, originally at the hole velocity (i.e., "refuse" from the hole), displaced by laser deceleration to a slightly lower velocity and remaining in the field of view of the fluorescence monitor.

Figure 5 shows a typical cold hole and refuse peak velocity distribution (doublet) obtained when the cooling and repumping lasers are activated, and when up-down gating of the fluorescence signal is used. The hole velocity is at about 350 m/sec. The cold features are accompanied by residual broad optical pumping features that are produced during the nonresonant period, and some unremoved thermal background. Both effects presumably are due to imperfect cancellation by the up-down gating.

We find that we can position the doublet at more or less any desired velocity in the range of the thermal distribution by adjusting synchronously the cooling and

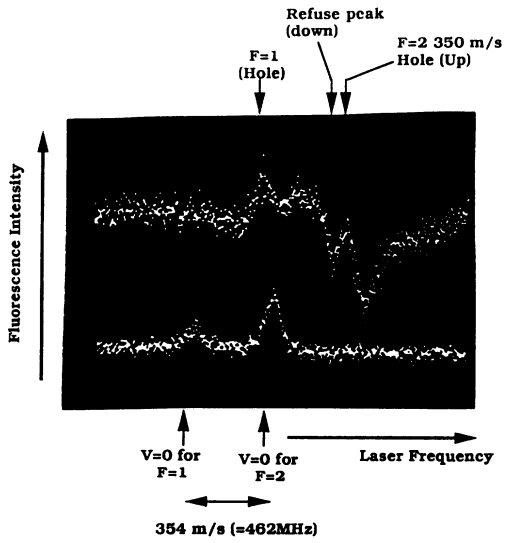

FIG. 5. Up-down signal averager velocity spectrum (upper trace) showing cold hole (at $\approx$350 m/s) and associated refuse peak. Signal is inverted so that a hole component gives a positive (upward) signal. The perpendicular calibration spectrum is also displayed (lower trace).

repumping laser tunings. Best operation (coldest features and highest refuse level) was found to occur with the repumping laser's intensity attenuated by about a factor of 10 below that of the cooling laser. (The ultimate low temperature of these features is undoubtedly complicated by our broad laser linewidth and the narrow spacing of the atom's upper-state hyperfine structure, whereupon our marginal probe laser's resolution and signal to noise ratio prevented a more detailed investigation of such effects.) At low-velocity tunings the refuse component significantly weakens in strength relative to the strength of the hole. The beam spatial profile's dependence on laser tuning (see below) indicates that this diminution of the refuse component at low velocity is due dominantly to its increased divergence at decreased velocity.

IV. VELOCITY HOLE-BURNING ATOMIC BEAM SPATIAL PROFILES

A second means for analyzing the beam was to measure the ac and dc atomic current lateral spatial profiles of the ribbon-shaped atomic beam by scanning a positively biased rhenium hot-wire detector across the beam's thin direction. The positive ion current produced by surface ionization of potassium on the wire is collected and amplified by an electrometer. Although the average dc signal, I_{dc}, of the detected atomic beam represents dominantly that due to a thermal velocity distribution, the cold (ac) component of the atomic beam is readily distinguishable from the thermal (dc) component through the use of an "up-down boxcar integrator" connected to the electrometer's output. Its operation is similar to that of a lock-in amplifier, except that the boxcar's integration is gated off and correspondingly ignores any current produced during the laser stabilization periods. During the resonant observation period, the signal is integrated with a positive sign, while during the nonresonant period, a negative sign is imposed. Since the dc component cancels and is thus ignored by the boxcar integrator, synchronous detection of only the ac component of the signal then has the effect of operation of the apparatus with two simultaneous beams—one a nearly monochromatic beam (ac) and the other a dominantly thermal beam (dc).

The phase-sensitive signal from the boxcar, I_{ac}, when positive represents an increase in atomic flux of atoms that is due to atoms interacting with the lasers, while, when negative, it represents a decreased atomic flux (i.e., the presence of holes) by such atoms. When the lasers are resonantly tuned, atomic beam cooling and deceleration occur. When the lasers are nonresonantly tuned, only optical pumping occurs, and a simple thermal beam is produced. The hot-wire current is neither sensitive to hyperfine state nor to atomic velocity, but only to total potassium flux. Thus any I_{ac} signal can only be due to a change in the spatial profile and/or intensity of the beam in response to the action of the cooling and repumping lasers.

Figures 6 and 7 show both the I_{ac} and I_{dc} lateral profiles taken at two different laser tunings. The tunings corresponding to hole velocities of 550 and 165 m/s, respectively. The I_{ac} profile shows the hole component

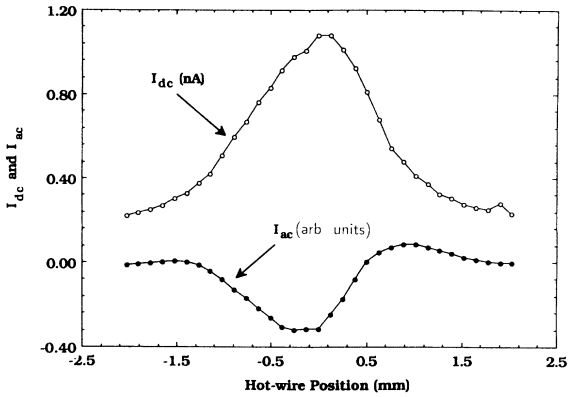

FIG. 6. I_{ac} and I_{dc} spatial profiles of a beam with a high-velocity (550 m/s) cold hole and associated refuse. Hole components are indicated by a negative I_{ac}.

(negative I_{ac}) with about the same width as that of the I_{dc} profile. It is surrounded on either side by the refuse component (positive I_{ac}), whose width is greater than that of the I_{dc} profile. The width is both qualitatively and quantitatively consistent with the expected perpendicular heating of the refuse component. The increased angular spread (increased lateral width and diminished height) of the refuse component's profile is determined by the ratio of the perpendicular heating average velocity to the parallel velocity of that component. Increasing divergence of the refuse component with decreasing velocity thus provides an effective lower limit of about 100 m/s to slow cold atomic beam potassium producible by this technique.

Slight asymmetries of the I_{ac} profiles relative to their associated I_{dc} profiles are also evident, especially in Fig. 7. Originally, the asymmetry was suspected to be due to a lack of parallelism between the atomic beam and the cooling or repumping laser beam. Although some of the asymmetry may be due to that effect, subsequent experiments (see Sec. VI, below) find it to be characteristic of a far more powerful effect. Moreover, we find that at various "resonant" laser tunings the asymmetry can become large and dominate the signal's dependence of laser tuning at a given stationary hot-wire position.

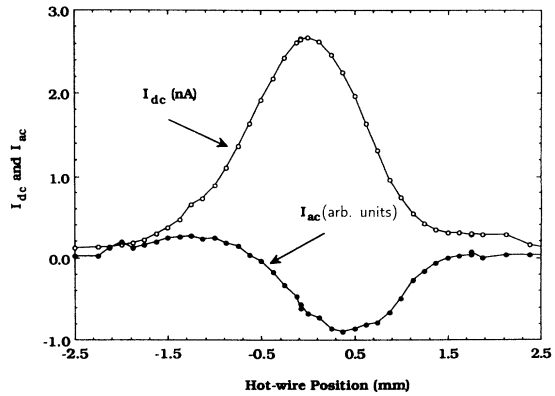

FIG. 7. Similar to Fig. 6 for low-velocity (165 m/s) cold hole and refuse. Note the lateral shift of the hole component relative to the refuse component.

V. DISCUSSION OF COOLING AND DECELERATION BY CONVENTIONAL METHODOLOGY

Given the spectacular success and popularity of conventional chirp (and Zeeman) cooling techniques in providing high flux sources of slow monoenergetic atomic beams for loading atom traps, it is seductive to assume that these methods are also useful as high intensity sources of these atoms. Thus seduced, we performed additional experiments wherein, during the resonant period, the laser frequencies were further frequency modulated with a kilohertz sawtooth ramp (chirped). Consistently with the observations by other workers, as the ramp amplitude increases above zero, the hole width is observed to increase and the refuse peak is shifted to low velocity. The refuse peak is thus decelerated (synchronously with the laser ramp) to its lower final velocity. One might naively hope that chirped operation will significantly increase the intensity of the refuse component as the chirp width is increased. On the contrary, negligible increase is found in response to a finite chirp width. At low final velocities the refuse component is still found to be vanishingly small. Based on the observed spatial profiles we conclude that the loss of intensity appears to be dominantly due to perpendicular heating.

We note that a quest for high beam intensity involves a quite different figure of merit from that needed for efficient loading of a trap. When the target volume for the beam (e.g., the atom trap) is large, then tight collimation of the output beam is relatively unimportant and a divergent low intensity (atoms crossing a unit area per sec per sterradian) broad beam is quite acceptable. Nonetheless, our experiments indicate that one-dimensional deceleration and cooling produces a very low beam intensity.

On the other hand, we note that the parent thermal beam is already very cold in the perpendicular directions by virtue of its geometric cooling by the collimating slits. Indeed, we observe that the intensity of holes in the parent beam is, in general, far higher (especially at low velocities) than that of the decelerated refuse components. The higher intensity is due to the fact that the hole beam maintains the perpendicularly cold collimation of the parent beam. Since our ac modulation technique effectively produces two simultaneous beams (ac and dc), the quasimonoenergetic holes can provide far more ac signal (albeit negative) at the hot wire than can the refuse atoms. Although an atom trap cannot profitably use a beam of holes, other applications, such as atom interferometry can. An added feature of the use of holes in the present geometry occurs at low velocity with the disappearance of the refuse, whereupon the hole intensity becomes monoenergetic.

A simple calculation suffices to conform our assertion. We first calculate the ratio of two quantities. For the numerator, we calculate the net flux of decelerated cold atoms, R_{chirp}, obtained by sweeping up atoms in the lower portion of a thermal distribution into a cold refuse peak by downward velocity chirping of a laser to a velocity, v_f. For the denominator, we calculate the number already in the thermal distribution at v_f for the same assumed effective laser bandwidth, Δv_{laser}. All laser frequencies are expressed here in terms of their equivalent Doppler velocity shift. The numerator of this ratio is then the number of atoms in the velocity interval between $v_f+\Delta v_{\text{chirp}}+\Delta v_{\text{laser}}/2$, and $v_f-\Delta v_{\text{laser}}/2$, while the denominator is the number in the same integral with Δv_{chirp} set to zero. For a thermal beam, this ratio is then given by

$$R_{\text{chirp}}=\frac{\int_{v_f-\Delta v_{\text{laser}}/2}^{v_f+\Delta v_{\text{chirp}}+\Delta v_{\text{laser}}/2} v^3\exp\left[-\frac{mv^2}{2kT}\right]dv}{\int_{v_f-\Delta v_{\text{laser}}/2}^{v_f+\Delta v_{\text{laser}}/2} v^3\exp\left[-\frac{mv^2}{2kT}\right]dv}.$$

Assuming an effective laser bandwidth of 20 m/s and a thermal potassium beam at 450 K, Fig. 8 displays this ratio as a function of Δv_{chirp} for various values of v_f.

Counterbalancing this gain, we must consider the loss in intensity that is due to the increased divergence of the refuse beam over that of the parent thermal beam. The profile of the parent thermal beam will be determined by its collimation angles, $\Delta\theta\times\Delta\phi$. If N photons are scattered by an atom during its transit through the laser beam, then the atom's perpendicular velocity will undergo a random walk in velocity space and accrue an increased divergence angle given by

$$\delta\theta,\delta\phi\approx\frac{N^{1/2}v_\gamma}{3^{1/2}v_p},$$

where v_γ is the velocity change for scattering one photon (1.3 cm/s for potassium), and v_p is the parallel velocity. The factor of $3^{1/2}$ assumes quasi-isotropic photon recoil. To burn a hole of width $\Delta v_{\text{chirp}}+\Delta v_{\text{laser}}$ in the thermal velocity distribution will require the scattering of

$$N=\frac{\Delta v_{\text{chirp}}+\Delta v_{\text{laser}}}{v_\gamma}$$

photons. Thus the intensity of the perpendicularly heat-

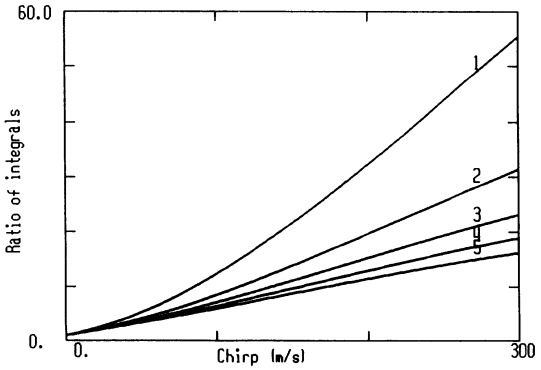

FIG. 8. The ratio R_{chirp} of atoms swept up in a thermal beam distribution by a downward velocity chirp, to the number already in the thermal distribution in the finite laser bandwidth, $\Delta v_{\text{laser}}=20$ m/s, as a function of chirp width Δv_{chirp}. Curves 1–5 are for $v_f=35$, 70, 105, 140, and 175 m/s, respectively.

ed beam component will be reduced relative to that of the hole component by the ratio

$$R_{\text{heating}} \approx \frac{\Delta\theta\Delta\phi}{\sqrt{\Delta\theta^2+\delta\theta^2}\sqrt{\Delta\phi^2+\delta\phi^2}} .$$

For a large target volume (such as that of an atom trap) that does not require tight collimation, i.e., one allowing large $\Delta\theta$ and $\Delta\phi$ then this ratio approaches one. On the other hand, for a highly collimated ribbon beam with small $\Delta\theta$, this ratio is quite small. For example, we plot R_{heating} as a function of Δv_{chirp} in Fig. 9 for the collimation parameters of our beam. The product, $R_{\text{chirp}} R_{\text{heating}}$, i.e., the net ratio of refuse to hole intensity, is plotted in Fig 10, also as a function of Δv_{chirp}. We see that for low-velocity cold beams, modest ramp lengths, and tightly collimated ribbon-shaped beams, the hole intensity will be significantly greater than the cooled refuse intensity, consistent with our observation.

Our consideration of the relevant orders of magnitude suggests an alternative scheme for producing an intense cold beam of atoms—that of velocity selection by simply deflecting atoms out of the parent beam with a small number of photons. Since the velocity change of a potassium atom upon scattering one $D2$ photon is about 1.3 cm/s, then to simply burn a hole 20 m/s ($\approx$26 MHz) wide requires the parallel momentum transfer corresponding to the scattering of about 1500 photons. Thus it is not surprising that doing so causes significant perpendicular heating—an average lateral broadening corresponding to $1500^{1/2} \approx 39$ photon momenta. On the other hand, a potassium atom moving at say 100 m/s requires only 10 photon momenta applied perpendicularly in the vicinity of the mirror to deflect it a hot wire's width ($\approx$1 mm) at the detector 1.3 m away. An atom thus deflected produces no signal. Hence direct transverse deflection of atoms can provide a much greater ac hot-wire signal per scattered photon than can longitudinal cooling accompanied by perpendicular heating. Moreover, by using velocity-selective deflection, the resulting perpendicular momentum spread (about three photon momenta) will be comparable to that obtained through the use of polarization-gradient molasses.

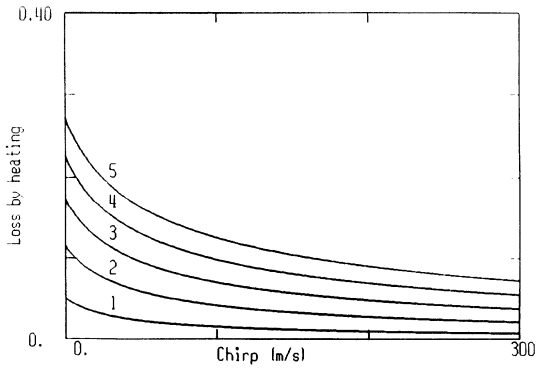

FIG. 9. Relative reduction of the intensity, R_{heating}, of the decelerated beam component (for our collimation geometry) caused by perpendicular heating, as a function of chirp width Δv_{chirp}. Curves 1–5 are for $v_f = 35$, 70, 105, 140, and 175 m/s, respectively.

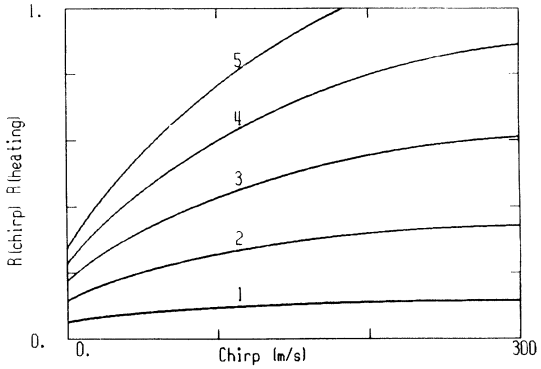

FIG. 10. The product $R_{\text{chirp}} R_{\text{heating}}$ showing the ratio of the intensity of the decelerated perpendicularly heated refuse beam component to that of the perpendicularly cold hole component, plotted as function of Δv_{chirp}. Curves 1–5 are for $v_f = 35$, 70, 105, 140, and 175 m/s, respectively.

This observation may seem surprising. Given the paucity of atoms available at low velocities in a thermal distribution, intuitively, one might expect velocity selection to be the least effective means for producing high intensity at low velocity. However, counter to this intuition the above calculation indicates that it provides a higher intensity at low velocities than does conventional chirp cooling. Thus, if transverse molasses is not employed, velocity selection is the preferred method for producing moderately low-velocity cold beams.

VI. CROSSOVER RESONANCES

Given the lateral asymmetry of the light in the small volume where it is incident on the mirror we now recognize that scattering of only a few photons there can give rise to significant lateral asymmetry to any cold atomic beam passing through this volume. Since this asymmetry can have a significant effect on the observed hot-wire signal, it is now not surprising that the refuse cold beam exhibited an observed asymmetry.

We further note that atoms in a so-called "cycling transition" are particularly strongly influenced by any such asymmetry. In ^{39}K a cycling transition occurs when σ^+ (or σ^-) light is applied to the transition $4s\,^2S_{1/2}(F=2) \rightarrow 4p\,^2P_{3/2}(F=3)$. In such a case $4s\,^2S_{1/2}(F=2)$ atoms are not immediately optically pumped out of their lower state. Instead, they can "cycle" many times before indirectly "leaking" into a $4s\,^2S_{1/2}(F=1)$ state. As a result, excitation by a single resonant laser frequency is sufficient to deflect them off of the hot wire to thereby produce a significant I_{ac} signal.

To investigate further the processes occurring only in the vicinity of the mirror we reconfigured the geometry from that of Fig. 11(a) to that of Fig. 11(b), wherein scattering of photons can occur *only* in the vicinity of the mirror. We then directed circularly polarized parallel light at *only one laser frequency* on the slit. The light was ac modulated (as described above) by closing a liquid crystal shutter during the nonresonant excitation period. Now, laser light thus crosses the beam at the mirror's

face, but does not counterpropagate along the atomic beam.

For this configuration Fig. 12 shows the I_{ac} signal produced and its dependence on laser tuning. For these data the hot wire is centered on the parent dc beam. Two broad peaks are evident on either side of the $F=2$, $v=0$ tuning position. The features in this signal are illuminated by reference to Fig. 13, in which we plot the Doppler shifted resonance positions for atoms at various atomic velocities against the associated (single) frequency of the laser. To simplify our discussion, we temporarily neglect energy differences among upper-state hyperfine structure levels, as these are only marginally resolvable by our laser bandwidths. Four excitation modes can occur for the various combinations of atomic hyperfine level and reflected or incident light. Each mode is tracked by a line

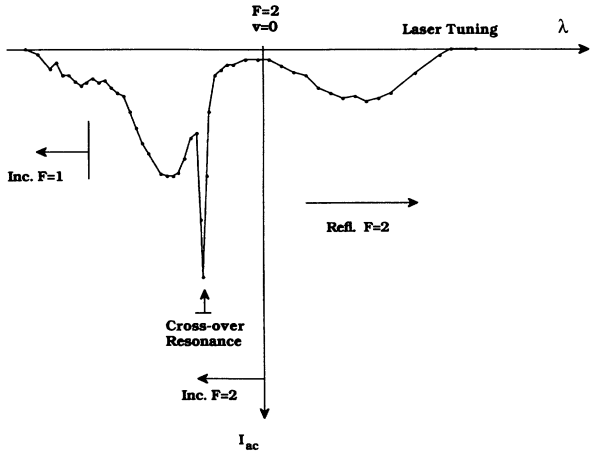

FIG. 12. I_{ac} signal produced by one-laser excitation using the geometry of Fig. 11(b), as a function of laser tuning. Negative I_{ac} corresponds to more deflected atoms (i.e., fewer detected atoms).

on this plot. Referring to both figures, we can see that the right-hand broad peak of Fig. 12 is produced by cycling $F=2$ atoms in the thermal beam that have been deflected away from the hot wire by light reflected off the mirror. The left-hand broad peak is produced by velocity-selected $F=2$ thermal atoms similarly deflected by light incident on the mirror. At lowest wavelengths, a second weak broad bump appears on the left-hand tail. It corresponds to noncycling $F=1$ atoms being deflected by incident light. The difference in widths of the two thermal peaks is due to the fact that the incident light is 60° away from parallel to the beam and has less Doppler shift than that of the reflected light which is only 32° away from antiparallel to the beam.

A sharp resonance is evident in the left-hand broad

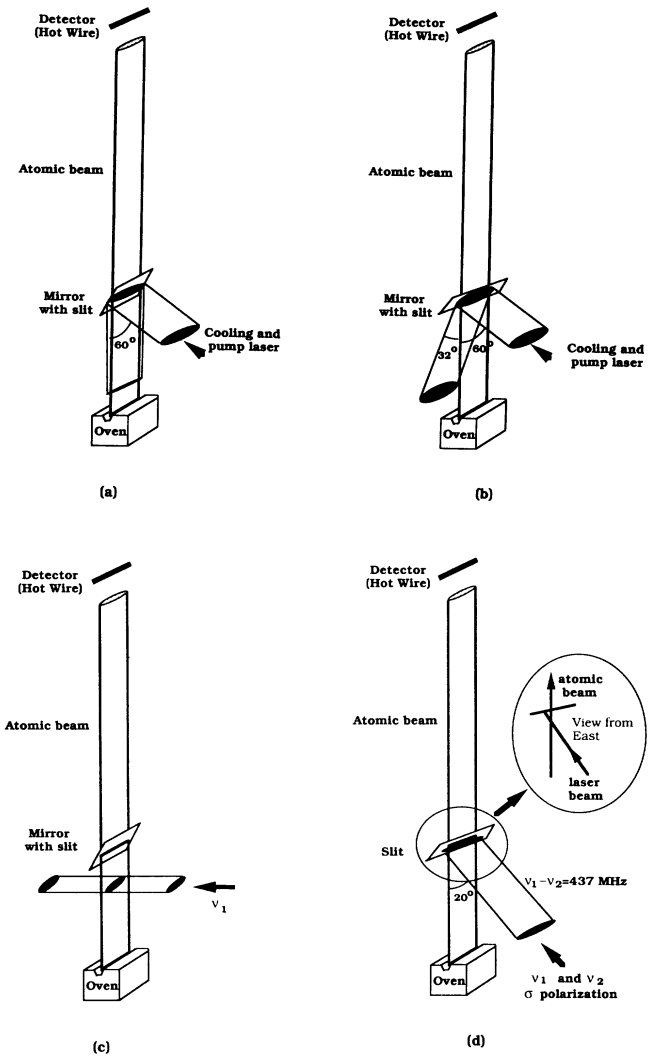

FIG. 11. (a) Geometry of the oven, mirror, and laser optics for the experiments described in Sec. II–IV. (b) Geometry used to explore the effects of crossover resonances occurring in the vicinity of the mirror. (c) Geometry allowing calibration of the lasers and high-resolution spectroscopy. (d) Geometry used for producing velocity-selected low-velocity beams. When the slit is nonreflecting, then one-laser crossover resonances disappear.

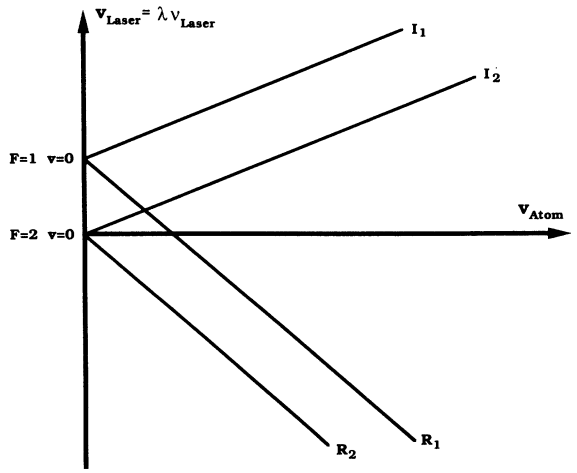

FIG. 13. Map of resonances in the space of laser frequency and atomic velocity. Excitation of $F=1$ and 2 atoms by incident and reflected light occurs on the four lines shown, which correspond to the geometry of Fig. 11(b). Line labeled R_1, for example, designates reflected light exciting $F=1$ atoms. A crossover resonance occurs at the intersection of R_1 and I_2 lines.

peak. It is due to 223 m/s $4s\ ^2S_{1/2}(F=2)$ atoms being excited by the incident light, being optically pumped to the $4s\ ^2S_{1/2}(F=1)$ level, whereupon light in the reflected beam is resonant to excite them. Thus such atoms do not rely on self-cycling of the $F=2$ atoms, but instead are pumped back and forth between the $F=1$ and 2 levels, and thereby scatter many photons during their transit through the laser light. Their signal is thereby enhanced roughly threefold over that produced by self-cycling atoms at the same velocity.

The origin of the crossover resonance is also evident from Fig. 13. It occurs when a line associated with excitation of $F=1$ atoms intersects a line associated with excitation of $F=2$ atoms. The slope of each line depends on the associated geometric inclination of the laser beam. The slopes are bounded above and below by $+1$ and -1, respectively, corresponding to antiparallel reflected and parallel incident light, respectively. (Perpendicularly incident light will correspond to a zero slope.) The geometry of the experiment thus determines the position of the crossover resonance. For the geometry associated with the data of Fig. 12 it involves the deflection of atoms at 223 m/s.

When two copropagating laser frequencies are used in the geometry of Fig. 11(b), then additional cycling resonances are possible. With two laser frequencies, one frequency excites $F=1$ atoms at a given velocity, while the second excites atoms with the same velocity in the $F=2$ level. A large number of two-laser cycling resonances are possible. Again neglecting upper-state hyperfine level energy differences, Fig. 14 presents a map of the two-laser frequency space and shows the loci of the possible resonances.

We investigated the spectral locations of the two-laser resonances experimentally by modulating only one of the two lasers with a liquid crystal shutter and searching for a resonance in the detected current when the other laser frequency was adjusted. An ac resonance is indicated by a negative I_{ac} signal, indicating an increased hole current. We were successful in locating resonances corresponding to all of the branches shown in Fig. 14. When the lasers are tuned to excite a two-laser resonance involving atoms near the peak of the thermal distribution, then an I_{ac} resonance is found, along with a simultaneous dip in I_{dc}. These resonances are sufficiently strong that they can be used to set the relative tunings of the two lasers.

A final comment is worth making. The presence of a mirror with a slit is not needed for crossover resonances to occur. Given the above analysis we expect such resonant deflections to occur whenever two laser beams and a collimated atomic beam cross at the same spatial position, and when the lasers are tuned so that the atoms can be pumped back and forth in response to the two Doppler shifted applied laser frequencies (i.e., whenever the atoms can undergo so-called Λ transitions).

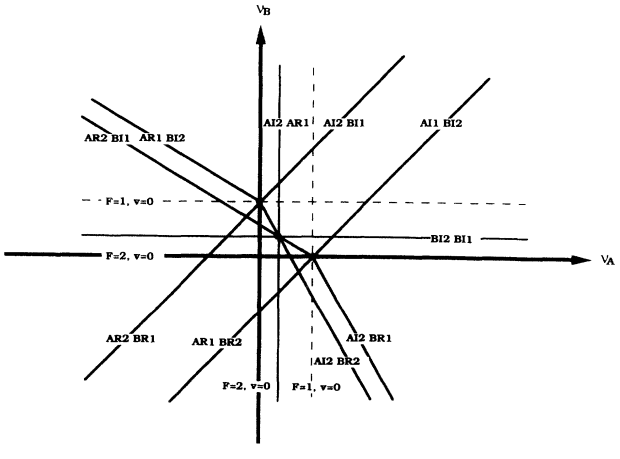

FIG. 14. Map of the two-laser frequency (ν_A and ν_B) space, for the configuration of Fig. 11(d), showing the loci of one- and two-laser resonances. The label AR1BI2, for example, indicates excitation of atoms in the $F=1$ level by laser A's reflected beam and of atoms at the same velocity in the $F=2$ level by laser B's incident beam.

VII. VELOCITY-SELECTIVE DEFLECTION

Our discussion in Sec. V indicates that a low-velocity beam with a high intensity of holes is available by simple hole burning. We also anticipate from this discussion that a comparably high intensity of cold monoenergetic atoms is also available by velocity-selective deflection. To test this idea further, in a third set of experiments we rearranged our optics to the configurations shown in Figs. 11(c) and 11(d) and replaced the mirror with a nonreflecting slit. We can switch between these two arrangements by manipulating mirrors outside of the vacuum chamber.

Using the perpendicular incidence arrangement of Fig. 11(c), we excited the atoms with only one (circularly polarized) laser frequency, ac intensity modulated with a liquid crystal shutter. This configuration then allows us to calibrate that laser's wavelength. Figure 15 shows the resulting I_{ac} signal obtained as a function of laser tuning. Three sharp peaks are evident. We identify these as corresponding (from right to left) to the unresolved ^{39}K transition $4s\ ^2S_{1/2}(F=1)\rightarrow 4p\ ^2P_{3/2}(F=0,1,2)$, to the ^{41}K cycling transition $4s\ ^2S_{1/2}(F=2)\rightarrow 4p\ ^2P_{3/2}(F=3)$, and to the ^{39}K cycling transition $4s\ ^2S_{1/2}(F=2)$

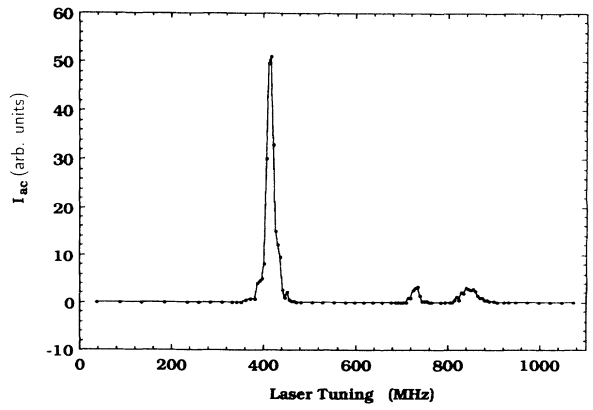

FIG. 15. I_{ac} signal produced as a function of laser tuning by deflecting the beam with one circularly polarized laser frequency, using the geometry of Fig. 11(c).

$\rightarrow 4p\ P_{3/2}(F=3)$. The ^{39}K transitions $4s\ ^2S_{1/2}(F=2) \rightarrow 4p\ ^2P_{3/2}(F=1,2)$ further provide a weak unresolved bulge to the lower right side of the left feature. Consistent with this identification, we note that the cycling transitions are stronger and narrower relative to those that do not cycle. This effect then allows the 6% abundant ^{41}K cycling transition (middle) to occur as strongly as the noncycling ^{39}K transition (right-hand side). Since cycling picks out only one line of the unresolved upper-state hyperfine multiplet, the cycling transitions are correspondingly narrower.

It is noteworthy that the right-hand peak is produced by noncycling atoms which immediately optically pump after scattering only one or two photons. The method demonstrated here thus allows very sensitive high-resolution spectroscopy.

When the arrangement of Fig. 11(d) is employed, we thus expect no crossover resonances. In contrast to the spectrum shown in Fig. 12, under one-laser excitation the right-hand thermal peak and the crossover resonance indeed disappear, as the reflected beam has now been removed. The left-hand broad feature remains. Correspondingly, we find that its associated ac signal is further enhanced by using excitation by two crossover resonant laser frequencies, thus inducing cycling.

Figure 16 plots as a function of calculated atomic velocity the resulting ratio of the ac hole current (on axis) to total incident dc current $(-I_{ac}/I_{dc})$ for excitation in the configuration of Fig. 11(d), with two circularly polarized laser frequencies. The experimental data points are plotted as diamonds. These data were taken using high laser power. The resolution of the beam's thermal distribution is now increased over that of Fig. 12. We attribute the increase to a laser incidence angle closer to parallel.

For comparison, we also plot in Fig. 16 the hole current calculated from an overly simplified model that assumes 100% deflection efficiency, independent of laser tuning. We take the effective parallel velocity equivalent laser bandwidth to be a constant, 12 m/s (adjusted slightly for the finite laser inclination). At most velocities the model overestimates the measured ac current. Most of the deficit is presumably related to a less than complete spatial separation of the deflected (positive I_{ac}) and hole (negative I_{ac}) beams. Indeed, data taken at reduced power show a progressive loss of hole current at increasing velocity, thereby yielding a peak current at a velocity less than that of the thermal beam's peak velocity.

On the other hand, at low velocity the simple model underestimates the ac current, where a second departure from the simple model presumably dominates. At low velocity one expects a broadening of the effective laser bandwidth to be caused by atoms spending greater time in the excitation volume. So doing, even the weak broad Lorentzian wings scatter photons and thereby create holes. Since it takes only a few scatterings to remove an atom from the beam, the net effect is to produce a hole velocity profile that is broader than that of the laser's bandwidth, and hence an increase in the observed hole current at low velocity. For our ≈ 10 nA detected dc beam, at 100 m/s the effective ac (low velocity) atomic surface spectral brightness (surface brightness per unit velocity interval) of our collimating slit is then about 3.6×10^{18} atom $m^{-2}s^{-1}sr^{-1}(m/s)^{-1}$, where again we have assumed (possibly optimistically) a parallel velocity spread of 12 m/s.

Using the geometry of Fig. 11(d) we measured the spatial profiles of the beam under excitation by two fixed laser frequencies. The incident laser power here is less than that used to obtain the data of Fig. 16. The resulting I_{ac} and I_{dc} profiles are shown in Figs. 17 and 18. The data for these figures are for laser tunings that excited atoms at 188 and 295 m/s, respectively. In both cases holes are burned in the parent beam's (dc) profile. The scattered atoms are seen to be pushed to the left and reappear as a cold-atom beam. In Fig. 17, the cold-atom beam is fully spatially separated from the parent dc beam (and from the ac hole beam) and may be isolated by additional collimation.

We note that the average deflection angle appears to scale with laser power and also to scale inversely with the square of the velocity. The first velocity factor is due to the kinematics, while the second is due to the increased time that slower atoms have to scatter photons. Profiles

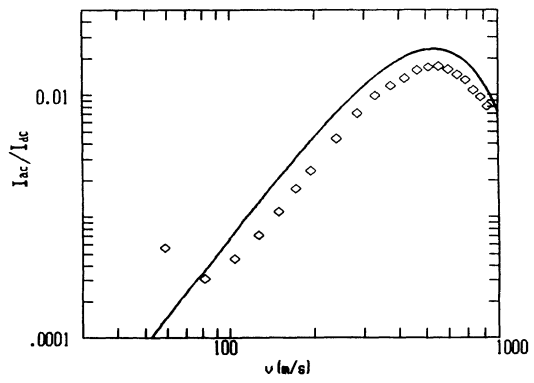

FIG. 16. Ratio of hole current (negative) to thermal atomic current, $-I_{ac}/I_{dc}$, as a function of deflected beam velocity for the geometry of Fig. 11(d).

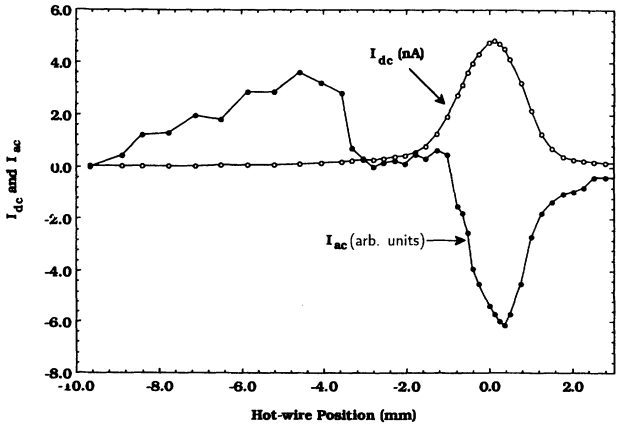

FIG. 17. I_{ac} and I_{dc} spatial profiles of the beam for two-laser velocity selection of 188 m/s $F=2$ atoms.

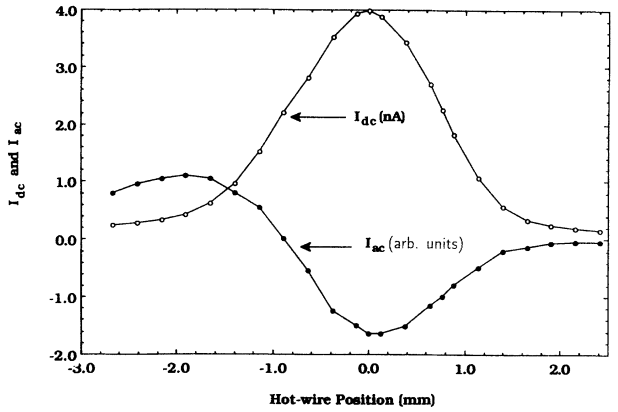

FIG. 18. Same as Fig. 17 for deflection of 295 m/s atoms.

measured at velocities lower than those shown in Figs. 17 and 18 with high laser power deflected the scattered cold-atom component out of the scan range of the hot wire, leaving only the hole component evident. For low-velocity excitation when the laser power is further reduced (by application of neutral density filters), then the cold-atom component is recovered.

In this arrangement, the diagonal incidence of the laser has two effects. The parallel component provides Doppler velocity selectivity, while the perpendicular component provides perpendicular momentum transfer for the deflection. Highest Doppler selectivity occurs at acute angles. When cycling is promoted by two-frequency excitation, the average perpendicular momentum transfer obtained at a given velocity and laser power is independent of the incidence angle. This is due to canceling factors of the sine of this angle. The average momentum transfer per scattered photon is proportional to the sine of the angle, while the time that an atom is illuminated is inversely proportional to the sine of the angle. Given the low required laser intensity, the parallel momentum transfer provides a parallel velocity change that is much less than that associated with the natural width of the transition.

With velocity-selective deflection we are able to produce comparably intense slow cold beams of both atoms and holes, as is seen in Fig. 17. For an application as a low-velocity source for an atom interferometer, use of the cold-atom beam is preferable to that of the cold hole beam, since in the latter case the presence of the copropagating strong dc thermal beam increases the detector shot noise. The cold-atom beam is nearly as intense as the cold hole beam because the deflection needed to separate the positive intensity beam from the parent beam thermal beam requires the scattering of only a handful of photons, whereupon the increased beam divergence associated with perpendicular heating is minimal and may be kept comparable to that of the parent beam, as well as comparable to that producible by polarization-gradient molasses. As a result, modestly high cold-atom intensity can be achieved, at low velocity, despite the paucity of atoms available at the low-velocity end of the thermal distribution.

VIII. SUMMARY AND CONCLUSIONS

We have explored the limitations associated with using conventional spontaneous-force slowing and cooling in combination with the use of diode lasers to produce slow cold potassium beams, and without the simultaneous application of perpendicular molasses cooling. We find that for velocities at the lower end of the thermal distribution the associated perpendicular heating provides a serious limitation to beam intensity producible by the use of this method. Both theoretically and experimentally we find that velocity selection provides a higher beam intensity. To this end, we describe a simple method for producing cold slow atomic beams, whose perpendicular velocity spread is comparable to that achievable with the use of polarization-gradient molasses. It can be used with only one low-power unnarrowed diode laser applied to a cycling transition, or with two such lasers applied to a non-cycling transition for a species with atomic ground-state hyperfine structure. For production of medium-velocity beams of atoms with no cycling transition, the use of a crossover resonance even allows production of cold beams using only one laser frequency. The method's alignment requirements are simple and far less critical than those required by conventional techniques. A simple reconfiguration of the laser optics may be performed outside of the vacuum chamber to allow *in situ* calibration of the laser wavelengths. While the intensity produced by this method may not compare with that available from other molasses-based systems, its requirements for laser power, number of laser frequencies, narrowness of laser bandwidths, etc. are considerably simpler to achieve.

ACKNOWLEDGMENTS

The authors wish to acknowledge enthusiastic help on this project from Matthias Reinsch and Glen Garfein. This work was supported by ONR Grant No. N00014-90-J-1475 and J. F. Clauser & Assoc., Walnut Creek, CA.

[1] See, for example, J. F. Clauser, in *Proceedings of the International Workshop on Matter-Wave Interferometry in the Light of Schrödinger's Wave Mechanics, Vienna, 1987* [Physical B **151**, 262 (1988)].

[2] R. N. Watts and C. E. Wieman, Opt. Lett. **11**, 291 (1986); C. E. Wieman and L. Hollberg, Rev. Sci. Instrum. **62**, 1 (1991).

[3] J. Nellessen *et al.*, J. Opt. Soc. Am. B **6**, 2149 (1989); F. Riehle *et al.*, Appl. Phys. B **54**, 333 (1992); E. Riis *et al.*, Phys. Rev. Lett. **64**, 1658 (1990).

[4] See, for example, M. Kasevich and S. Chu, Phys. Rev. Lett. **67**, 181 (1991), and references therein for an application of this method to provide a source of slow atoms for use in atom-interferometry experiments.

[5] F. Shimizu *et al.*, Phys. Rev. A **46**, 17 (1992), and (unpublished).

[6] Cooling and trapping of rubidium and cesium (see Ref. [1]) have been done using diode lasers, and sodium and more recently lithium have likewise been done with dye lasers. For our atom-interferometry application, we chose to use potassium by virtue of its moderately low mass and long de Broglie wavelength, along with its accessibility by diode lasers. A preliminary version of this work was presented by the authors in Bull. Am. Phys. Soc. **38**, 1135 (1993).

[7] R. C. Miller and P. Kusch, Phys. Rev. **99**, 1314 (1955).

[8] It is noteworthy that a pronounced hole (interference minimum) is observed to be formed in the beam by evident diffraction effects if the mirror faces on opposite sides of the slit are not accurately in the same plane.

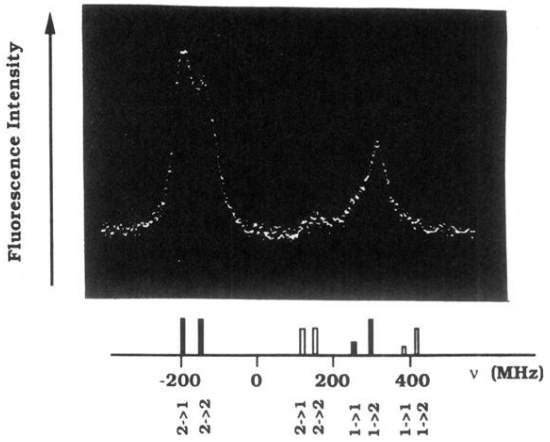

FIG. 3. Upper trace: $D1$ fluorescence spectrum observed at perpendicular crossing used for probe laser calibration. Lower trace: Wavelength reference values for ^{39}K (solid) and ^{41}K (open).

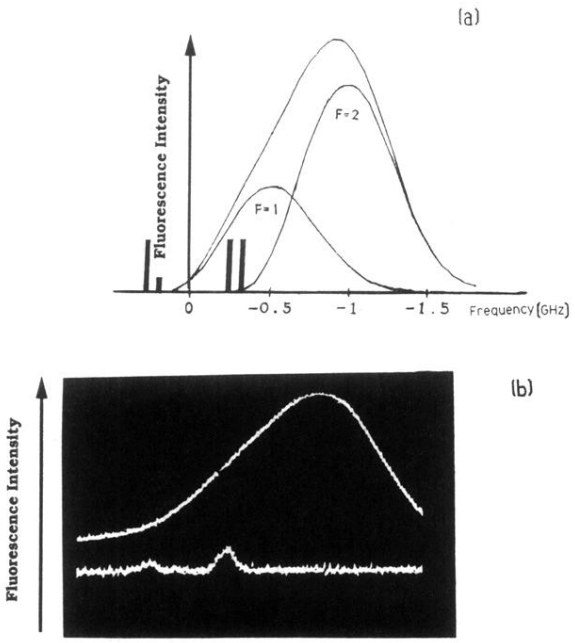

FIG. 4. Thermal parent beam velocity spectrum (a) calculated, and (b) observed in the near-parallel fluorescence with no cooling lasers incident (upper trace), along with the associated perpendicular spectrum used for velocity calibration (lower trace).

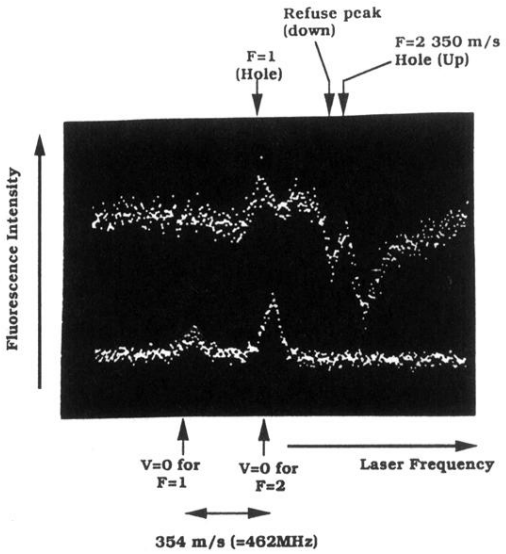

FIG. 5. Up-down signal averager velocity spectrum (upper trace) showing cold hole (at $\approx$350 m/s) and associated refuse peak. Signal is inverted so that a hole component gives a positive (upward) signal. The perpendicular calibration spectrum is also displayed (lower trace).